

# Open boundary conditions in stochastic transport processes with pair-factorized steady states

Hannes Nagel<sup>a</sup>, Darka Labavić<sup>b</sup>, Hildegard Meyer-Ortmanns<sup>b</sup>, Wolfhard Janke<sup>a</sup>

<sup>a</sup>*Institut für Theoretische Physik, Universität Leipzig, Postfach 100 920, 04009 Leipzig, Germany*

<sup>b</sup>*School of Engineering and Science, Jacobs University Bremen, P.O. Box 750561, 28725 Bremen, Germany*

---

## Abstract

Using numerical methods we discuss the effects of open boundary conditions on condensation phenomena in the zero-range process (ZRP) and transport processes with pair-factorized steady states (PFSS), an extended model of the ZRP with nearest-neighbor interaction. For the zero-range process we compare to analytical results in the literature with respect to criticality and condensation. For the extended model we find a similar phase structure, but observe supercritical phases with droplet formation for strong boundary drives.

*Keywords:* stochastic transport processes, pair-factorized steady states, open boundary conditions

---

## 1. Introduction

Stochastic mass transport processes such as the asymmetric simple exclusion process (ASEP) or the zero-range process (ZRP) proposed by Spitzer (1970) are simple transport models for particle hopping to improve the understanding of basic phenomena in the dynamics of particles in driven diffusive systems. Generally these particles are abstract and may represent objects from the microscopic to the macroscopic scale depending on the situation and their specific dynamics. Just as these particles and their interactions, the underlying spatial structure is an important factor in adapting and mapping these models to physical processes. In this work we will consider two such processes, that feature the formation of particle condensates in periodic systems driven far from equilibrium. We are interested in studying these processes in a situation, where the system is driven by the flux of particles entering and leaving through open boundaries. First we look into the zero-range process, where we can compare our numerical results with analytic predictions available from the literature. Then we discuss the effect of open boundaries on the condensation phenomenon for an extended transport process with short-range interactions as realized by the pair-factorized steady states (PFSS) model introduced by Evans (2006) and Waclaw et al. (2009a, 2009b).

## 2. Zero-range process

The basic stochastic mass transport process of particle hopping consists of a gas of indistinguishable particles on a one-dimensional lattice with  $L$  sites. Every site  $i$  can be occupied by any number of particles  $m_i$ . In the zero-range process, in every time step of the discrete stochastic time evolution, a random site  $i$  is selected, where a single particle may leave to a neighbor with the hopping rate  $u(m_i)$ . That is, particles only interact with other particles on the same site. The direction of the hop is determined randomly, often with respect to rates that introduce asymmetric dynamics. For an overview of different dynamics we refer, to the book by Schadschneider et al. (2011) or the review by Schütz (2001).

In this work we shall consider the model with hopping rates  $u(m) = 1 + b/m$  on a one-dimensional lattice with open boundary conditions also discussed by Evans (2000) and Kafri et al. (2002). Under periodic boundary conditions, the

---

*Email addresses:* Hannes.Nagel@itp.uni-leipzig.de (Hannes Nagel), D.Labavic@jacobs-university.de (Darka Labavić), H.Ortmanns@jacobs-university.de (Hildegard Meyer-Ortmanns), Wolfhard.Janke@itp.uni-leipzig.de (Wolfhard Janke)

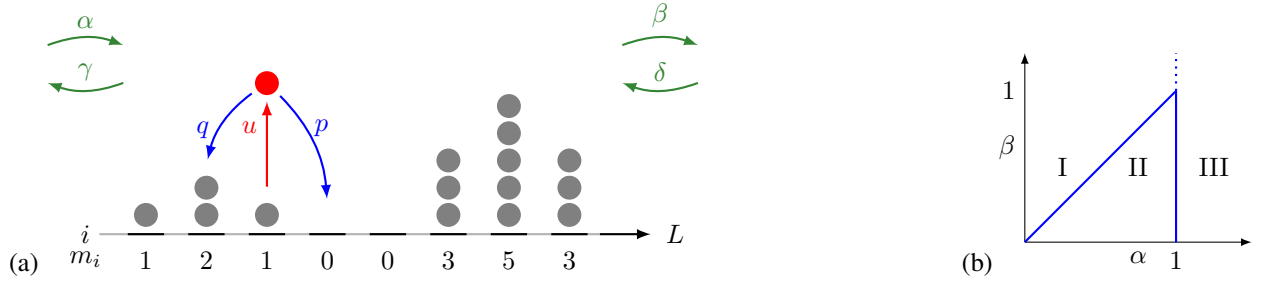


Figure 1: (a) Schematic representation of the zero-range process on a one-dimensional lattice with  $L$  sites and particle injection (rates  $\alpha, \delta$ ) and removal (rates  $\gamma, \beta$ ) through open boundaries at sites  $i = 1, L$ . (b) Phases induced by boundary drive in the discussed transport processes. A description of the phases is given in the sections of the respective transport process.

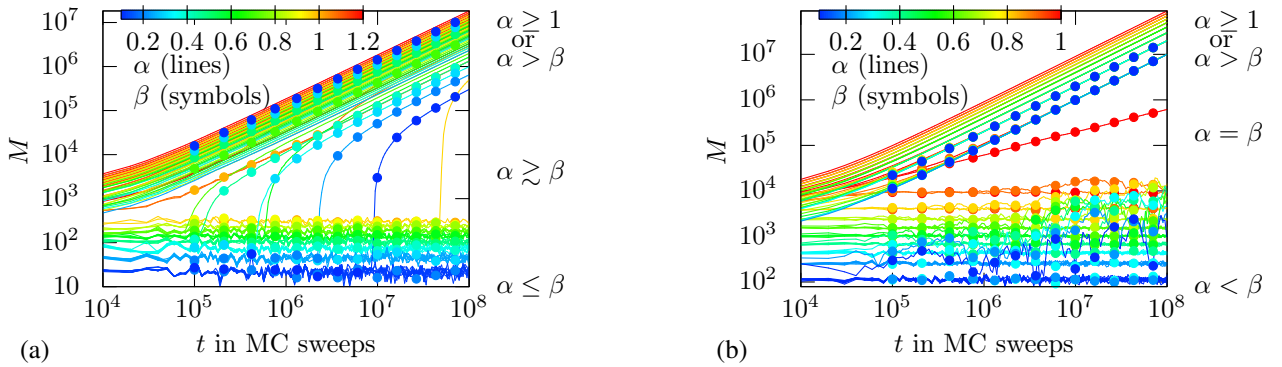


Figure 2: The time evolution of the total number of particles  $M = \sum_{i=1}^L m_i$  for the (a) ZRP and (b) PFSS transport models shows the distinct differences between phases I, where a steady state exists, and phases II and III. Line color indicates boundary rates for particle injection  $\alpha$  ( $= \delta$ ), symbol color that of particle removal  $\beta$  ( $= \gamma$ ). The system size is  $L = 1024$  sites.

main feature of this model is the formation of a single-site condensate consisting of all particles exceeding a critical density  $\rho_c = 1/(b-2)$  for  $b > 2$  such that all other sites have an average occupation equal to  $\rho_c$ . Effects of open boundaries on this process have been studied analytically by Levine et al. (2005), to which we shall first compare our results before we continue to an extended model. Particle exchange at the boundaries at the first (last) site is achieved by injection with rates  $\alpha$  ( $\delta$ ) and removal with rates  $\gamma$  ( $\beta$ ), respectively, as illustrated in Fig. 1(a).

In the analytic study by Levine et al. (2005), local fugacities are determined using a quantum Hamiltonian approach proposed in Schütz (2001) to find the phase structure given in Fig. 1(b) and respective properties of the phases with respect to the boundary rates: Phase I, for  $\alpha \leq 1, \alpha \leq \beta$ , is the only phase, where the system has a steady state. The total number of particles  $M = \sum_{i=1}^L m_i$  remains stable, the occupation number distribution becomes  $P(m_i = m) = \alpha^m / m^b$  and the resulting particle density in the bulk system is subcritical,  $\rho_{\text{bulk}} < \rho_c$ . In phase II, for  $\alpha \leq 1, \alpha > \beta$ , the rate of particle influx outweighs that of outflux and particles pile up at the boundary site(s) before leaving, forming one or two condensates in the totally asymmetric ( $p = 1, q = 0$ ) or symmetric ( $p = q = 1/2$ ) cases, respectively. Condensation specific properties in the bulk are not analytically determined. In phase III, for  $\alpha > 1$ , the rate of particles entering at the boundary site(s) exceeds the maximal possible hopping rate so that particles pile up on the boundary site(s) after entering the system and the total number of particles grows linearly in time.

We will compare only to the cases where the injection and removal rates at each boundary are equal in the symmetric process,  $\alpha = \delta$  and  $\beta = \gamma$ , and  $\gamma = \delta = 0$  for the totally asymmetric case. In both cases we use the hopping parameter  $b = 5$ .

By numerical simulation these phases and properties are easily reproduced and visible in observables such as the total number of particles  $M$  over time as shown in Fig. 2(a) with the same phase boundaries as predicted. A more detailed look at the criticality of the system with respect to the boundary drive is possible by computing the bulk density deep inside the system as shown in Fig. 3 for the (a) totally asymmetric and (b) symmetric processes. In the totally asymmetric case, the condensate on the last site in phase II cannot contribute to the bulk density which

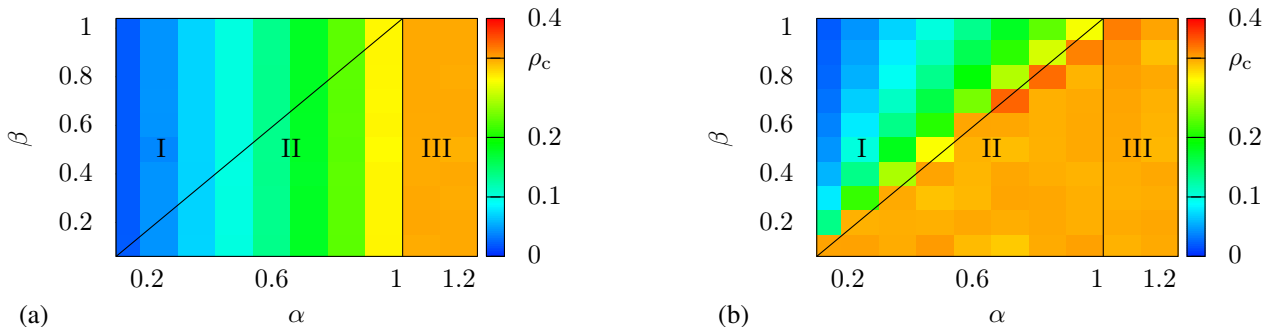


Figure 3: Bulk densities  $\rho_{\text{bulk}}$  of the (a) totally antisymmetric and (b) symmetric ZRP with  $\alpha = \delta$ ,  $\beta = \gamma$  and hopping parameter  $b = 5$  averaged over time for various values of boundary rates  $\alpha, \beta$ . The black lines indicate the phase transition lines. In phase III of the totally asymmetric case and phases II and III of the symmetric case, the bulk density becomes equal to the critical density  $\rho_c = 1/3$ . The system size is  $L = 1024$  sites.

remains low and subcritical. In phase III, a particle condensate forms at the first site acting as a reservoir for the bulk of the system that becomes critical ( $\rho_{\text{bulk}} = \rho_c = 1/(b-2) = 1/3$ ) as it acts like the bulk in a periodic system with a condensate. In contrast, in the symmetric system in both phases II and III these condensates form at the two boundary sites and particles may hop back into the system, so that the bulk becomes critical already for  $\alpha > \beta$  in phase II. Very small droplets of several particles become visible in the bulk, but the monotonic falloff of the distribution of occupation numbers in the phases II and III confirms the absence of condensates in the bulk.

### 3. Stochastic transport with nearest-neighbor interactions and pair-factorized steady state

An interesting extension of the ZRP is the introduction of nearest-neighbor interactions: spatially extended condensates are observed for periodic lattices in the model proposed by Evans et al. (2006), where the condensation process is qualitatively similar to that of the zero-range process. We will consider a slightly different model with hopping rates

$$u(m_i|m_{i-1}, m_{i+1}) = \frac{g(m_i - 1, m_{i-1}) g(m_i - 1, m_{i+1})}{g(m_i, m_{i-1}) g(m_i, m_{i+1})}, \text{ where } g(m, n) = \sqrt{e^{-m^c} e^{-n^c} e^{-|m-n|^b}} \quad (1)$$

is a two-point weight function that allows the tuning of the critical density as well as the condensate's width and shape between single-site, rectangular and smooth bell-like shapes as discussed by Waclaw et al. (2009a, 2009b) and Ehrenpreis et al. (2014). Instead of a fully factorized steady state as in the ZRP, this extended model has a pair-factorized steady state (PFSS). For an overview of the condensate shapes and other properties see Ehrenpreis et al. (2014). We choose this model to be able to also study the effects of open boundaries in the transition region between ZRP-like single-site condensates and extended shapes. However, in this work we first concentrate on a single specific parameterization,  $b = 1.2$ ,  $c = 0.6$ , where we know from previous work by Waclaw et al. (2009a, 2009b) and Ehrenpreis et al. (2014) that the periodic system exhibits smooth bell-like condensate shapes. The specific parameter point is chosen because of the comparably fast dynamics, low critical density and intermediate condensate extension.

Again, we can recognize the rough phase structure by determining the total number of particles  $M = \sum_{i=1}^L m_i$  in the system versus time and get a similar picture as for the ZRP in Fig. 2(b). For  $\alpha < 1$ ,  $\alpha < \beta$ ,  $M$  remains stable and linear growth of  $M$  is observed for  $\alpha > \beta$  as well as for  $\alpha \geq 1$ . Only directly at the transition between the phases I and II, for  $\alpha = \beta$ , an increase in the square root of time,  $M(t) \sim \sqrt{t}$ , is observed. Similar to the behavior of the ZRP near this transition line ( $\alpha \gtrsim \beta$ ), for lower boundary rates  $\alpha = \beta = \gamma = \delta$  the system may remain in the steady state of phase I for a long time with a stable total particle number and then suddenly jumps to the observed behavior. For  $\alpha > \beta$  as well as  $\alpha \geq 1$  linear growth is observed due to particles piling up on the boundary sites as for the ZRP.

To determine the effect of these boundary condensates on the state and the criticality of the bulk system, we computed the density  $\rho_{\text{bulk}}$  deep inside the system, droplet mass distributions and average occupation number profiles. The structure of the obtained bulk densities for various boundary rates as shown in Fig. 4 easily compares with that of the ZRP in Fig. 3. The phase structure is again visible looking at the totally asymmetric (Fig. 4(a)) and

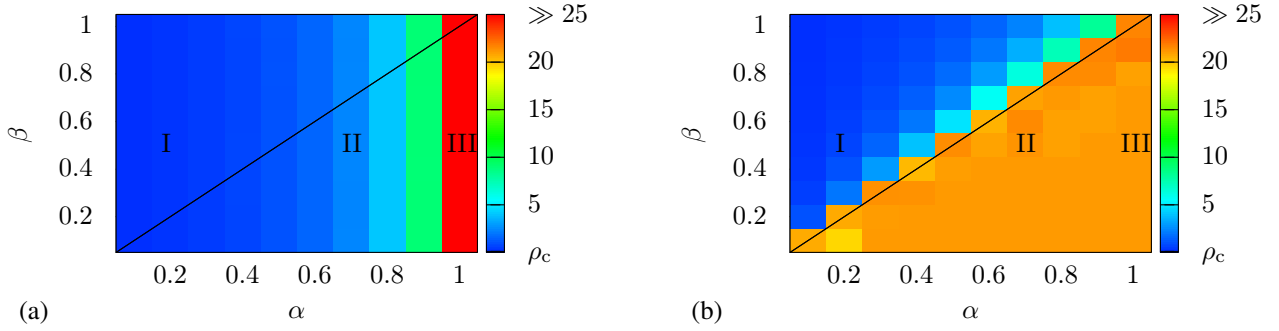


Figure 4: Bulk densities  $\rho_{\text{bulk}}$  of the (a) totally asymmetric and (b) symmetric PFSS (with  $\alpha = \delta, \beta = \gamma$ ) transport processes averaged over time for various values of boundary rates  $\alpha, \beta$ . Here the bulk densities become much larger than the critical density  $\rho_c \approx 0.11$  in phase III (totally asymmetric case) and phases II and III (symmetric case), respectively. The system size is  $L = 1024$  sites.

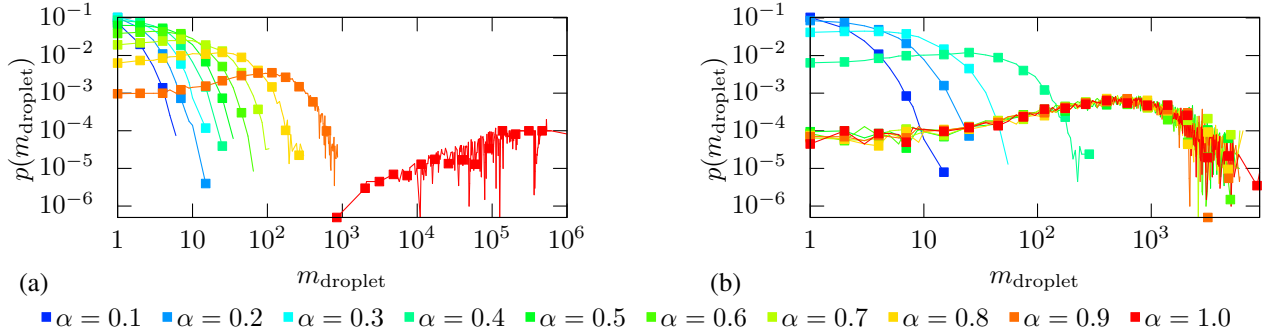


Figure 5: Droplet size distributions for the (a) totally asymmetric and (b) symmetric PFSS processes. Parameters range from  $\alpha = 0.1$  (blue) to  $\alpha = 1.0$  (red) with  $\beta = 0.5$  constant. For better readability the distributions have been binned.

symmetric (Fig. 4(b)) models. However, the average bulk density in phases II and III is clearly above the critical density  $\rho_c \approx 0.11$  as determined in Ehrenpreis et al. (2014) for the model on a periodic lattice, where rapidly emerging particle condensates would be expected. We also observe an increase of the average bulk densities with the square root of simulation time in phases II and III, while it is stable in the steady-state phase I. This growth in the bulk system can be easily understood when the system has a long-range correlation between sites deep inside the system and the boundary sites. In fact, we observe such long-range correlations in the average occupation numbers at one boundary site for the totally asymmetric process and at both boundary sites for the symmetric process.

The values of the bulk density above the critical density of the periodic system raise the question whether particle condensates are formed in the bulk system. To answer this question we first concentrate on the distribution of droplet masses in the bulk. In a system without condensation, this distribution is expected to fall off monotonically, while a bump in the tail indicates an excess of larger droplets as a product of the condensation process. For the totally asymmetric process (Fig. 5(a)) a shift to larger droplet masses for increasing  $\alpha$  in phases I and II due to an increasing bulk density is observed. The cause of the distinctively different distribution for  $\alpha = 1$  in this figure is that the bulk does not contain separated droplets but consists of highly occupied sites only. In the symmetric process (Fig. 5(b)) a similar shift to larger droplet masses is observed only in phase I. For  $\alpha \geq \beta$  the droplet mass distributions then collapse onto each other with a bump for large droplets. This is a strong indicator that indeed a condensation process takes place in the bulk of phases II and III. Since, in these phases, the number of particles in the system as well as the bulk density grow in time, this condensation process is likely stationary. That is, the droplets keep growing while the system evolves. In both cases, totally asymmetric and symmetric, a bump in the droplet mass distribution develops just before the transition lines ( $\alpha \geq 1.0$  and  $\alpha \geq \beta$ , respectively) are crossed. We interpret these as finite-size effects due to the limited distance of the bulk to the boundary sites.

## 4. Summary

We studied effects of open boundaries on condensation phenomena in the zero-range process (ZRP), reproducing the analytic results in Levine et al. (2005), and an extended transport process (1) with nearest-neighbor interactions. We found that boundary drive in the pair-factorized steady states (PFSS) model creates mostly the same phase structure as in the ZRP, with distinct behavior directly on the transition line between phases I and II. However, different properties are observed in phases II and III, where no steady state exists for the ZRP. Due to effective long-range interactions, the boundary drive is still visible deep inside the bulk of the system, increasing the particle density above its critical value, thus creating many large droplets but no well separated or even single condensates as in the periodic lattice model.

As an outlook to further research into this system, we would like to study specifically whether the tunable extended PFSS model (1) in the single-site condensate regime  $b < c$  maps onto the ZRP with respect to boundary drive effects and how the transition to extended rectangular and smooth bell-like shaped condensates is reflected by the discussed properties of the boundary drive. More specifically, does the sensitivity to the boundary depend on the shape of the extended condensate in the case of the PFSS model? It would also be of interest to elucidate how the lattice size influences the size of formed droplets via the time it takes for droplets to move to the boundary.

## Acknowledgements

We would like to thank the DFG (German Science Foundation) for financial support under the twin Grants No. JA 483/27-1 and ME 1332/17-1. We further acknowledge support by the DFH-UFA graduate school CDFA-02-07.

## References

- Ehrenpreis, E., Nagel, H., Janke, W., 2014. Numerical survey of the tunable condensate shape and scaling laws in pair-factorized steady states. *J. Phys. A: Math. Theor.* 47, 125001.
- Evans, M.R., 2000. Phase transitions in one-dimensional nonequilibrium systems. *Braz. J. Phys.* 1, 42–57.
- Evans, M.R., Hanney, T., Majumdar, S.N., 2006. Interaction driven real-space condensation. *Phys. Rev. Lett.* 97, 010602.
- Kafri, Y., Levine, E., Mukamel, D., Schütz, G.M., Török, J., 2002. Criterion for phase separation in one-dimensional driven systems. *Phys. Rev. Lett.* 89, 035702.
- Levine, E., Mukamel, D., Schütz, G.M., 2005. Zero-range process with open boundaries. *J. Stat. Phys.* 120, 759–778.
- Schadschneider, A., Chowdhury, D., Nishinari, K., 2011. *“Stochastic Transport in Complex Systems – From Molecules to Vehicles”*. Elsevier, Amsterdam.
- Schütz, G.M., 2001. Exactly solvable models for many-body systems far from equilibrium. In: *“Phase Transitions and Critical Phenomena”*, Vol. 19. Domb, C., Lebowitz, J.L. (Eds.). Academic Press, New York, Ch. 1, pp. 1–251.
- Spitzer, F., 1970. Interaction of Markov processes. *Adv. Math.* 5, 246–290.
- Wacław, B., Sopik, J., Janke, W., Meyer-Ortmanns, H., 2009a. Mass condensation in one dimension with pair-factorized steady states. *J. Stat. Mech.* P10021
- Wacław, B., Sopik, J., Janke, W., Meyer-Ortmanns, H., 2009b. Tuning the shape of the condensate in spontaneous symmetry breaking. *Phys. Rev. Lett.* 103, 080602.